ELSEVIER

Journal of Fluorine Chemistry 112 (2001) 241–246

JOURNAL OF FLUORINE CHEMISTRY

www.elsevier.com/locate/jfluchem

Synthesis and properties of neodymium containing oxide fluoride glasses

Masayuki Takashima*, Susumu Yonezawa, Tomoo Tokuno, Hidekazu Umehara, Takehisa Kato

Department of Materials Science and Engineering, Faculty of Engineering, Fukui University, 3-9-1 Bunkyo, Fukui 910-8507, Japan

Received 29 May 2001; accepted 31 August 2001

Abstract

New oxide fluoride glasses containing a large amount of Nd^{3+} were synthesized in NdF_3–AlF_3–GeO_2 and NdF_3–BaF_2–GeO_2 systems. The melting temperature was at 1200–1400 °C. The glass transition temperatures were 800–850 °C. The glasses synthesized in this study had the refractive indices (n) of 1.56–1.74, except for $25NdF_3{\cdot}12.5BaF_2{\cdot}62.5GeO_2$ glass having n of >1.77. The fluorine in the starting mixture tended to go away during the melting due to the sublimation of AlF_3 (or GeF_4) and the pyrohydrolysis of fluorides. The fluorine content of $40NdF_3{\cdot}20BaF_2{\cdot}40GeO_2$ glass (19.3 wt.%) decreased to 5 wt.% during melting due to sublimation of GeF_4 and pyrohydrolysis of the fluorides during melting. The maximal contents of Nd^{3+} in the glass were 63 and 58 cation% for NdF_3-AlF_3-GeO_2 and NdF_3-BaF_2-GeO_2 systems, respectively. The results suggest that fluorine was uniformly present in the glass network.

Keywords: Neodymium containing glass; Oxide fluoride; Germanium oxide; Three components system; Refractive index

1. Introduction

Host materials of optically active ions are required to be transparent and have high solubility of those ions. In general, both fluoride glasses and fluoride crystals are highly transparent materials and have higher rare earth ion incorporation. In actual, it is difficult to prepare the fiber forms of crystalline materials compared with vitreous materials. Glasses containing rare earth ions have been investigated as materials with various optical applications such as up-conversion lasers, fluorescent devices, non-linear optical devices, light amplifiers and so on [1–7]. A variety of matrices such as oxides, phosphates, fluorides and oxide fluorides have been studied to generate various optical properties [1–9]. In order to improve the optical properties of glasses or to find new functional materials, the new glass matrices have been studied to examined larger amounts of rare earth ions or to control the electronic states of rare earth ions in them. For example, traditional oxide glasses doped with small quantities of rare earth ions have been reported [10]. When rare earth ions are present in oxide glass matrices, it has been pointed out that the states of rare earth ions arising from the 4f electron configurations are little affected by the surroundings of the ions. In case of binary anion glasses, the effect of the glass matrices on rare earth ions could be controlled by their composition. Oxide fluoride glasses are one of the attractive cases for this.

We have reported the possibility of the oxide fluoride glass formation with large contents of rare earth ions and have established the reproducible procedure to prepare the LnF_3–MF_x–SiO_2 glasses [11]. Generally rare earth ions are doped into oxide glass matrices but the content of rare earth ions are <30 mol% as their fluorides. The LnF_3–MF_x–SiO_2 glasses can contain >60 mol% as LnF_3. The high contents of rare earth ions in the glasses may improve the optical properties or may exhibit new properties. In addition, the refractive indices tend to increase with an increase in the content of rare earth ion in the glasses. Evidently the kind of matrix influences on the optical properties of glasses. Because the bonding character of Nd–O is less ionic than that of Nd–F, oxide fluoride glass matrices may provide an unique environment which is not identical in oxide and fluoride matrices. In this study, NdF_3–MF_x–GeO_2 glasses ($MF_x = BaF_2$ or AlF_3) were attempted to be prepared and characterized. Especially the electronic state of fluorine in the glass was focused to understand the character of glass matrix.

2. Experimental

Anhydrous NdF_3 (3N) as a raw material was provided by Shin-Etsu Chemical Co. Ltd. AlF_3, BaF_2 (Guaranteed grade, Nakarai Chemical Co. Ltd.) and GeO_2 (5 N, Mitsuwa chemical Co. Ltd.) were used as the starting materials. The mixture of NdF_3, MF_x (BaF_2 or AlF_3) and GeO_2 were ground in an alumina mortar and dried under vacuum

* Corresponding author. Tel.: +81-776-27-8614; fax: +81-776-27-8614.
E-mail address: takashima@matse.fukui-u.ac.jp (M. Takashima).

0022-1139/01/$ – see front matter
PII: S0022-1139(01)00518-8

($<2 \times 10^{-3}$ Torr) for >12 h at 120 °C. The mixture was compacted into a platinum boat and set in an electric furnace filled with argon gas. The mixture was heated to 1200–1400 °C at a heating rate of 5 °C min^{-1}. After the melt was held at 1200 °C for 1 h, it was quenched by putting it onto molecular sieves cooled with liquid nitrogen. The quenching rate was approximately 120 °C s^{-1}. The products were observed by using an optical microscope (NIKON Optiphoto-2) and/or a scanning electron microscope (Hitachi S-800) and then characterized by means of X-ray powder diffraction (XRD; Shimadzu XD-3A, 30 kV, 20 mA, Cu Kα), X-ray photoelectron spectroscopy (XPS; Shimadzu ESCA-750, Mg anode), electron probe microanalysis (EPMA; Shimadzu EPMA-C1), X-ray fluorescence specrosopy (XFS; Shimadzu EDX-800) and differential thermal analysis (DTA; SII TG/DTA 32, Ar purge, RT −1200 °C, 10 °C min^{-1}). The fluorine content was determined from EPMA data by a ZAF (Z, atomic number effect; A, absorption effect; F, fluorescence effect) method. In EPMA analysis, Nd_2O_3, NdF_3, AlF_3, BaF_2 and GeO_2 were used as the standard samples. The ratios of Nd/Al/Ge and Nd/Ba/Ge after glass formation were measured with EPMA and XFS, respectively. The peak profile of F Kα in EPMA was measured at an acceleration voltage of 15 kV, a sample current of 30 nA and a probe diameter of 50 μm. The fluorine content was also measured by chemical analysis. The powdered sample was dissolved into fused KOH and then dissolved into water. The fluorine concentration in the solution was measured by using a F^- ion selective electrode. NdF_3 and BaF_2 were used as the standard samples. The refractive index was measured by the immersion method with standard solutions (Becke line method [12], $n = 1.50$–1.74, 0.01 step). The density was measured by using pycnometer with He gas (Micromertics AccuPyc 1330).

3. Results and discussion

3.1. Characterization

The XRD patterns of $80NdF_3{\cdot}10AlF_3{\cdot}10GeO_2$ (NAG811), $40NdF_3{\cdot}30AlF_3{\cdot}30GeO_2$ (NAG433) and $10NdF_3{\cdot}40AlF_3{\cdot}50GeO_2$ (NAG145) products which were melted at 1400 °C are shown in Fig. 1. NAG145 shows a number of sharp peaks in the XRD pattern. These peaks are mainly assigned to be due to the $Ge_2Al_6O_{13}$ crystal. Because the presence of neodymium was confirmed by EPMA, the unassigned peaks must correspond to some other phases containing neodymium. By the observation with an optical microscope, the NAG145 product has two different regions in which one region is transparent and the other is opaque. The needle-like crystal was observed in the opaque region. The transparent region exhibited very smooth surface, and no grain was observed in it. Such product may be regarded as a partially crystallized sample. There were no intense diffraction peaks in the XRD patterns of NAG811 and NAG433. However, several weak peaks were present in the XRD pattern of NAG811. The NAG811 product consisted of transparent and opaque regions as NAG145, while the NAG433 product was completely uniform and transparent. The opaque region of NAG811 must be crystalline. The peaks in the XRD pattern of NAG811 were not identical to those of NAG145, indicating that some other compounds except for $Ge_2Al_6O_{13}$ were formed in the product. However, the peaks were so weak that these were not definitely assigned. The NAG433 product with no peak in the XRD pattern and with complete transparency is classified as vitreous.

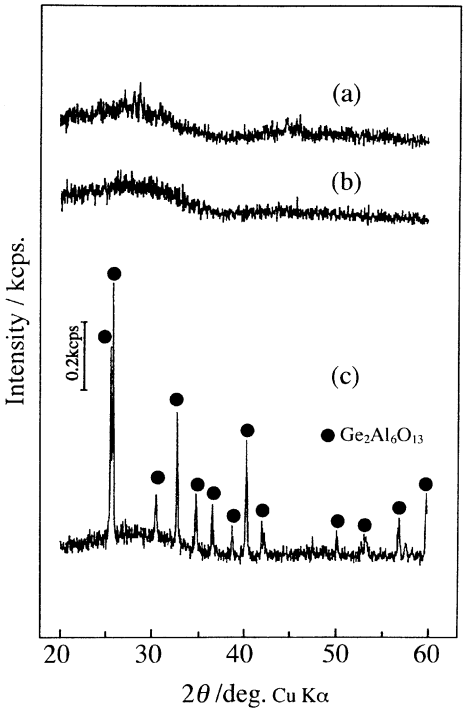

Fig. 1. XRD patterns of the NdF_3–AlF_3–GeO_2 products after melting at 1400 °C (with compositions of $80NdF_3{\cdot}10AlF_3{\cdot}10GeO_2$ (a), $40NdF_3{\cdot}30AlF_3{\cdot}30GeO_2$ (b) and $10NdF_3{\cdot}40AlF_3{\cdot}50GeO_2$ (c)).

3.2. NdF_3–AlF_3–GeO_2 system

Fig. 2 shows the glass-formation diagram in the NdF_3–AlF_3–GeO_2 system under the melting condition of 1400 °C. The glass formation was observed in a wide composition range. Glass was obtained even at the $70NdF_3{\cdot}10AlF_3{\cdot}20GeO_2$ composition which has very large content of neodymium. However, weight loss during melting at 1400 °C became *ca.* >10 wt.%. This weight loss might corresponds to the amount of all fluorine in the starting mixture. Fluorine might have gone away as HF during the melting by pyrohydrolysis. In order to examine the fluorine contents of the products, EPMA measurements were carried out (Fig. 3). The fluorine contents were 6.18, 2.03 and 0.43 wt.% for $50NdF_3{\cdot}40AlF_3{\cdot}10GeO_2$, $30NdF_3{\cdot}60AlF_3{\cdot}10GeO_2$ and $10NdF_3{\cdot}20AlF_3{\cdot}70GeO_2$ products while the fluorine contents in stating mixtures were 35, 40 and 15 wt.%, respectively.

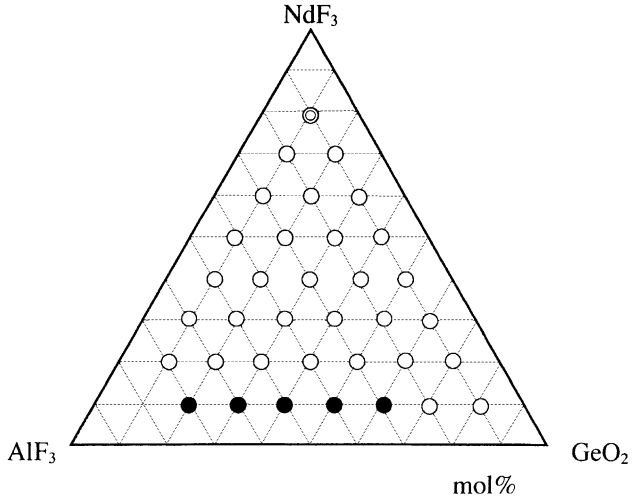

Fig. 2. Glass-formation diagram in the NdF_3–AlF_3–GeO_2 system. Open circle, double circle and closed circle mean vitreous, partially crystallized and crystallized products, respectively. The melting was carried out at 1400 °C.

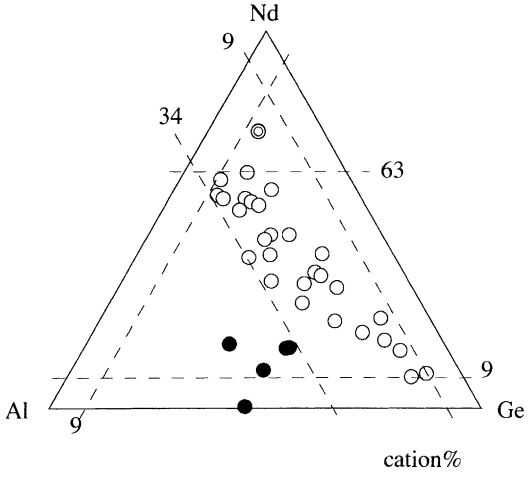

Fig. 4. Glass-formation diagram in NdF_3–AlF_3–GeO_2 system with composition analyzed by EPMA. Open, double and closed circles mean vitreous, partially crystallized and crystallized products, respectively. The melting was carried out at 1400 °C.

Large amount of fluorine must vaporize as HF and/or AlF_3. However, the fluorine still remain in the products while the fluorine content must be smaller than nominal one. Fig. 4 shows the glass-formation diagram represented by cation composition analyzed by means of EPMA. The compositions of the products are greatly different from those of the starting compositions. Especially, the aluminum content-tends to decrease during melting. This is due to sublimation of AlF_3 during melting since it begins to be sublimated at 700 °C [13]. The sublimation of AlF_3 also causes a decrease in the fluorine content in the product. Around 60% of fluorine is lost during melting by the pyrohydrolysis and sublimation of AlF_3. The actual composition range in which the glass products are obtained is narrower than that expected from nominal compositions for the NdF_3–AlF_3–GeO_2 system under the present melting condition. The oxide fluoride glass with 63 mol% NdF_3 as a maximal content was able to be synthesized in this system, while the composition of the glass product was difficult to be controlled due to the sublimation of AlF_3 during melting process. In order to avoid the sublimation of AlF_3, the melting temperature was attempted to be lowered. When the melting temperature was lowered, the composition range of glass-formation reduced. No glass product was obtained at temperatures <1150 °C. Even at the temperature, the sublimation of AlF_3 was not completely avoided. It has been reported that the aluminosilicate glasses containing rare earth element exhibit high glass-transition temperature of 850–900 °C [14]. The oxide fluoride glasses obtained here also exhibited high glass-transition temperatures ranging from 800 to 850 °C.

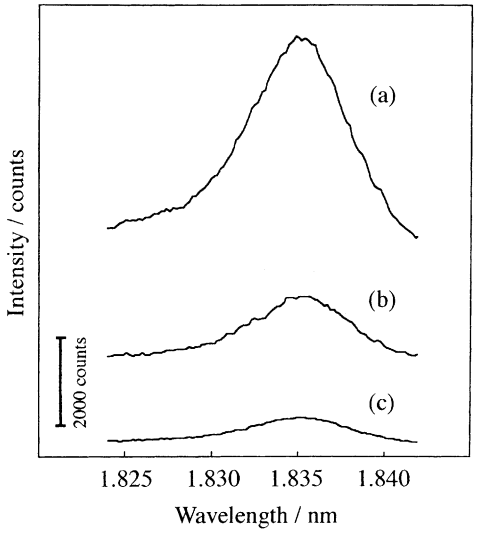

Fig. 3. EPMA profile of F Kα in $50NdF_3{\cdot}40AlF_3{\cdot}10GeO_2$ (a), $30NdF_3{\cdot}60AlF_3{\cdot}10GeO_2$ (b) and $10NdF_3{\cdot}20AlF_3{\cdot}70GeO_2$ (c) glasses.

3.3. NdF_3–BaF_2–GeO_2 system

Fig. 5 shows the glass-formation diagram in the NdF_3–BaF_2–GeO_2 system in nominal compositions after melting at 1200 °C. The glass formation range in the figure was narrower than that in the NdF_3–AlF_3–GeO_2 system in Fig. 4. This may be because BaF_2 does not act as a network-forming component, while AlF_3 is a typical component to form glass-network. The weight loss during melting was <7 wt.%. The glass-formation diagram represented by cation composition analyzed by using XFS is shown in Fig. 6. Only a slight change in composition during melting was detected in the NdF_3–BaF_2–GeO_2 system, while much larger change was detected in the NdF_3–AlF_3–GeO_2 system. If 10 wt.% of Ge in GeO_2 in $40NdF_3{\cdot}20BaF_2{\cdot}40GeO_2$ mixture sublimes from the melt as GeF_4 and oxide ions are left in the melt, the weight loss during melting should be 4 wt.%, i.e., the fluorine content of the $40NdF_3{\cdot}20BaF_2{\cdot}40GeO_2$ glass should be 18 wt.%. Since the fluorine content of the $40NdF_3{\cdot}20BaF_2{\cdot}40GeO_2$ glass was determined to be 5 wt.% by EPMA measurement, pyrohydrolysis of the fluorides must

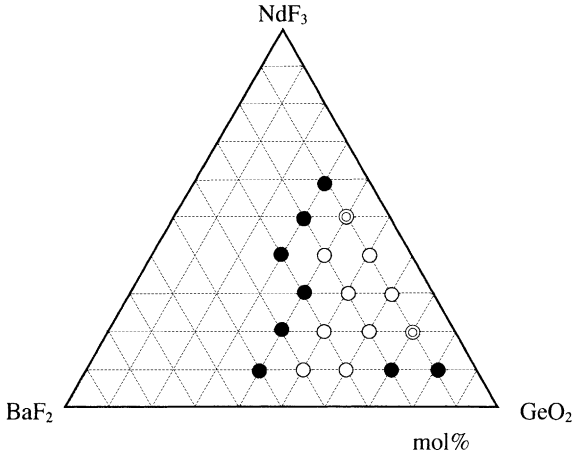

Fig. 5. Glass-formation diagram in NdF_3–BaF_2–GeO_2 system with nominal compositions under melting at 1200 °C. Open circle, double circle and closed circle mean vitreous, partially crystallized and crystallized products, respectively.

take place in NdF_3-BaF_2-GeO_2 system while total weight loss was reduced rather than in case of NdF_3-AlF_3-GeO_2 system. The fluorine amount lost during melting cannot be explained by only the sublimation of GeF_4. The pyorohydrolysis of fluorides must take place simultaneously. Anyway the composition of the melt was stabilized by using BaF_2 instead of AlF_3 and the glass products were obtained in the composition range of 10–40 mol% NdF_3, 10–40 mol% BaF_2 and 40–70 mol% GeO_2. Fig. 7 shows absorption spectra of $10NdF_3 \cdot 30BaF_2 \cdot 60GeO_2$ (a) and of $40NdF_3 \cdot 10BaF_2 \cdot 50GeO_2$ (b) between 300 and 800 nm. These spectra are very similar to each other and have the typical profile for the compound containing Nd^{3+}. The peaks around 340 and 600 nm, however, are a little different from each other. The peaks around 520 nm are well separated in two, while these peaks in the spectrum of barium crown glass are overlapped with each other. The state of Nd^{3+} in the glasses may depend on the content of Nd^{3+} and/or the composition of the glass-network.

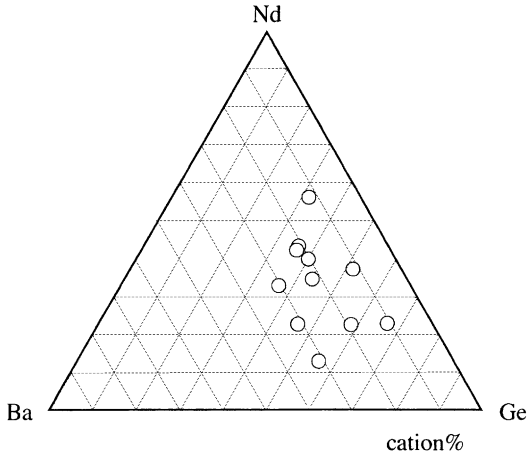

Fig. 6. Glass-formation diagram in NdF_3–BaF_2–GeO_2 system in cation composition analyzed by using XFS. Only the glass samples are shown.

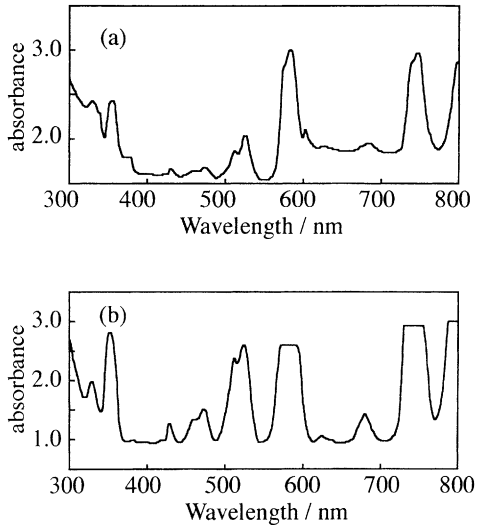

Fig. 7. Absorption spectra of $10NdF_3 \cdot 30BaF_2 \cdot 60GeO_2$ (a) and of $40NdF_3 \cdot 10BaF_2 \cdot 50GeO_2$ (b) between 300 and 800 nm.

3.4. Density and refractive index

Fig. 8 shows the relationship between the density (d) and the refractive index (n) of the oxide fluoride glass samples prepared. The linear relationship was observed between d and n in the d region of 2–4. The solid line in Fig. 8 is expressed as follows;

$$n = 0.17d + 1.00 \quad (1)$$

In general, it has been known that the linear $n-d$ relationship holds for glass samples [15]. The values for a quartz glass

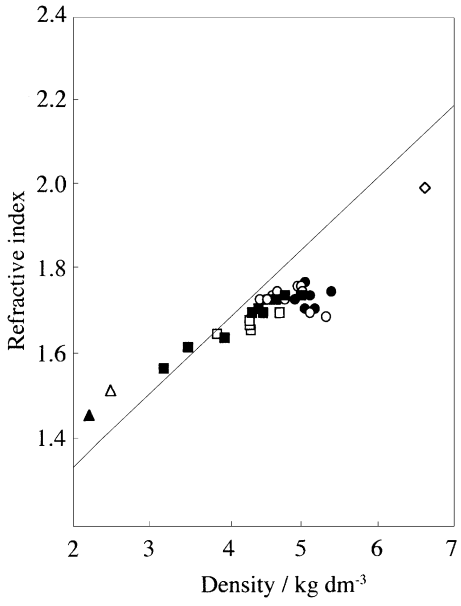

Fig. 8. Relationship between density and refractive index in oxide fluoride glass samples (closed circle; NDF_3-BaF_2-GeO_2, open circle; NdF_3-AlF_3-GeO_2, closed square; NdF_3-Al_2O_3-SiO_2 and open square; NdF_3-AlF_3-SiO_2 systems). The values for quartz glass (closed triangle) [15], borosilicate glass (open triangle) (Iwaki Glass Co., COVER 18-18) and $60PbO \cdot 21.3WO_3 \cdot 16.1P_2O_5 \cdot 1.6CdO \cdot 1.0TiO_2$ glass (open diamond) [16] are also shown.

(closed triangle) [16] and a borosilicate glass (open triangle) (Iwaki Glass Co., COVER 18-18) are also plotted in the figure. These typical glasses also satisfy Eq. (1). The value of $60PbO{\cdot}21.3WO_3{\cdot}16.1P_2O_5{\cdot}1.6CdO{\cdot}1.0TiO_2$ glass (open diamond) [17] is plotted as an example with the highest refractive index. The relation between n and d deviates from Eq. (1) for d values >4.5. In addition, the n values scatters. It was difficult to find an appropriate expression for the relationship between n and d in the region of $d > 4.5$. It seemed that lower BaF_2 content gives higher refractive indices in the NdF_3–BaF_2–GeO_2 system. Generally, the relation between n and d is expressed as

$$n - 1 = \frac{R}{V} = \left(\frac{R}{M}\right)d \quad (2)$$

where R, V and M are polarizability, molecular volume and molecular weight, respectively. Evidently, Eq. (1) is a derivative from Eq. (2). When R decreases, n becomes small even with the same density of glass. The polarizability of the glass sample might be reduced by Ba^{2+} in this case. It has been reported that it was difficult to obtain the glasses with very high refractive index (>1.8) with divalent ions like Ba^{2+} [18]. Such discussion is impossible in the NdF_3–AlF_3–GeO_2 system because the composition was greatly changed due to AlF_3 sublimation during melting. There are the samples which have higher refractive indices than 1.74, e.g. $25NdF_3{\cdot}12.5BaF_2{\cdot}62.5GeO_2$ (NBG215) and $40NdF_3{\cdot}10BaF_2{\cdot}50GeO_2$. Especially, the refractive index of NBG215 glass sample is >1.77. The measurement of the refractive index over 1.77 was experimentally difficult in this study. The glasses with very high refractive indices of near or over 1.8 may be synthesized with this oxide fluoride system. Since the optical properties of rare earth ions may be affected, useful information about the synthesis of a new functional glass material may be given.

3.5. State of fluorine in the glass

There are some reports that the EPMA peak profiles of F Kα in some metal fluorides are affected by their bonding states [19–21]. Fig. 9 shows the EPMA peak profiles (open circles) of F Kα in the $40NdF_3{\cdot}20BaF_2{\cdot}40GeO_2$ (a) and $40NdF_3{\cdot}40AlF_3{\cdot}20GeO_2$ (b) glasses. Dashed and dotted lines indicate the F Kα profiles of NdF_3 and BaF_2 (or AlF_3), respectively. The peak profile of F Kα in the batch material (before melting) of $40NdF_3{\cdot}20BaF_2{\cdot}40GeO_2$ is also shown in Fig. 9a (solid circles). Assuming an additive property, the solid lines are calculated as the summation of these two lines in the NdF_3/BaF_2 (or AlF_3) ratio of 4:2 (a) and 4:4 (b). In the NdF_3–BaF_2–GeO_2 system, full width at half maximum (FWHM) of the peak was smaller than that calculated from the batch material, although the maximum peak position was well expressed by the average (the observed value, 1.833 nm; the calculated value, 1.834 nm; the starting material value, 1.834 nm). This suggests that fluorine is uniformly present in the glass network because

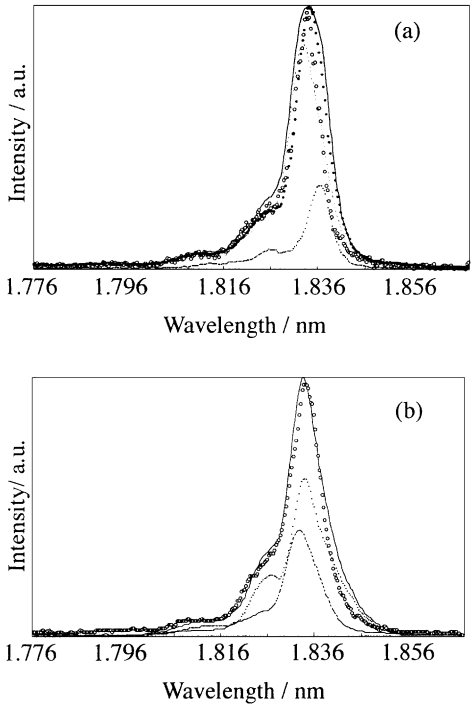

Fig. 9. EPMA peak profiles (open circles) of F Kα in $40NdF_3{\cdot}20BaF_2{\cdot}40GeO_2$ (a) and $40NdF_3{\cdot}40AlF_3{\cdot}20GeO_2$ (b) glasses. Dashed and dotted lines indicate NdF_3 and BaF_2 (or AlF_3) profiles, respectively. Closed circles in (a) indicates $40NdF_3{\cdot}20BaF_2{\cdot}40GeO_2$ starting mixture.

the peak should become wider when the two kinds of fluorine (F in NdF_3 and BaF_2) exist. Although the difference in FWHM between the calculated peak and the observed one for NdF_3–AlF_3–GeO_2 system was smaller than that in NdF_3–BaF_2–GeO_2 system, FWHM of the peak of glass is still larger than the calculated one. In this system also, therefore, fluorine must be uniformly present in the glass network. The satellite peak can be seen at wavelength shorter than the maximum peak position ($K\alpha_{1,2}$) in Fig. 9a and b. This satellite peak is due to the F $K\alpha_{3,4}$ transition [19]. It has been suggested that when the bonding character shifts to ionic, the ratio of the intensities of the maximum peak and that of this peak becomes larger. $K\alpha_{3,4}/K\alpha_{1,2}$ in Fig. 9b is larger than that in Fig. 9a. This fact reveals that the environment around fluorine is more ionic in the NdF_3–AlF_3–GeO_2 system than in the NdF_3–BaF_2–GeO_2 system.

4. Conclusion

Oxide fluoride glasses containing Nd^{3+} were able to synthesize in the NdF_3–AlF_3–GeO_2 system (melting at 1200–1400 °C) and the NdF_3–BaF_2–GeO_2 system (melting at 1200 °C). In the NdF_3–AlF_3–GeO_2 system, the sublimation of AlF_3 remarkably occurred and the compositions of the glasses were largely different from those of the starting mixtures. In the NdF_3–BaF_2–GeO_2 system, the compositions of glasses were slightly different from those of the

starting mixtures although the sublimation of GeF_4 took place. In both systems, the pyrohydrolysis of the fluorides in the mixture took place. The fluorine contents were lowered by the sublimation of AlF_3 (and/or GeF_4) and pyrohydrolysis of fluorides during melting. The fluorine content of $40NdF_3{\cdot}20BaF_2{\cdot}40GeO_2$ glass (19.3 wt.%) decreased to 5 wt.%. Glass transition temperatures of the oxide fluoride glasses were 800–850 °C. The refractive indices of the glasses were around 1.7. Considering the relation between density and refractive index in the oxide fluoride glasses, a variety of circumstances for Nd^{3+} may be generated by using this type of oxide fluoride glass matrix. Therefore, these glasses may have various optical applications.

Acknowledgements

This study was supported by a Grant-in-Aid for Exploratory Research from The Ministry of Education, Science, Sports and Culture of Japan.

References

[1] A. Kaminskii, Laser Crystals, Their Physical and Properties, Springer, New York, 1990.
[2] Y. Wang, J. Ohwaki, Appl. Phys. Lett. 63 (1993) 3268.
[3] F. Auzel, D. Pecile, D. Morin, J. Electrochem. Soc. 122 (1975) 101.
[4] M.J. Dejneka, J. Non-Cryst. Solids 239 (1998) 149.
[5] E.R. Taylor, B.N. Samson, D.W. Hewak, J.A. Medeiros Neto, D.N. Payne, S. Jordery, M. Naftaly, A. Jha, J. Non-Cryst. Solids 184 (1995) 61.
[6] T. Iqbal, M.R. Shahriari, P. hajcak, G.H. Sigel Jr., L.R. Copeland, W.A. Reed, Appl. Opt. 33 (1994) 965.
[7] S.A. Payne, W.F. Krupke, B.H.T. Chai, J. Opt. Soc. Am. B11 (1994) 2054.
[8] M. Syojiya, M. Terumoto, R. Kanno, Y. Kawamoto, J. Ceram. Soc. 107 (1999) 419.
[9] M. Poulain, M. Poulain, Mater. Sci. Forum 67/68 (1991) 129.
[10] K. Sun, W.-H. Lee, W.M. Risen Jr., J. Non-Cryst. Solids 92 (1987) 145.
[11] T. Kato, M. Takashima, S. Yonezawa, W. Sugiyama, in: Proceedings of the Abstract of The 18th Fluorine Conference of Japan, Vol. 1, 1993, pp. 1–2.
[12] P.F. Kerr, Optical Mineralogy, McGraw-Hill, New York, 1959.
[13] D.R. Lide (Ed.), CRC Handbook of Chemistry and Physics, 78th Edition, CRC press, Boca Raton, New York, 1997–1998.
[14] J.E. Shelby, J.T. Kohli, J. Am. Ceram. Soc. 73 (1990) 39.
[15] T. Izumitani, Optical Glasses and Laser Glasses, Nikkan Kogyo Shinbun, Tokyo, 1998.
[16] R.B. Sosman, The Properties of Silica, Reinhold, New York, 1927.
[17] J.J. Rothermel, K.H. Sun, A. Silverman, J. Am. Ceram. Soc. 32 (1949) 153.
[18] E.H. Hamilton, O.H. Grauer, E. Zabawsky, C.H. Hahner, J. Am. Ceram. Soc. 31 (1948) 132.
[19] H. Takahashi, I. Minato, Y. Kondo, Jpn. J. Appl. Phys. 37 (1998) 2070.
[20] O. Benka, R.L. Watson, R.A. Kenefick, Phys. Rev. Lett. 47 (1981) 1202.
[21] D.S. Urch, J. Chem. Soc., Chem. Commun. (1982) 526.